

MODELING OF SELF-HEALING PHENOMENA IN A POLYMER MATRIX BASED ON A MICROCAPSULE SYSTEM

S. Specht¹, J. Bluhm² and J. Schröder³

Institute of Mechanics, University of Duisburg-Essen
Universitätsstr. 15, 45141 Essen, Germany

¹e-mail: steffen.specht@uni-due.de, web page: <http://www.uni-due.de/mechanika/>

²e-mail: joachim.bluhm@uni-due.de, web page: <http://www.uni-due.de/mechanika/>

³e-mail: j.schroeder@uni-due.de, web page: <http://www.uni-due.de/mechanika/>

Key words: Theory of Porous Media, Self-Healing, Phase Transition

Abstract. In this contribution we focus on the numerical simulation of self-healing polymer composites using the Theory of Porous Media (TPM). The model consists of four different phases: solid matrix material with embedded catalysts, liquid healing agents, solid healed material and air. The amount of catalysts inside the matrix is described by their local concentration. For the description of damage behavior, a discontinuous damage model is used. Furthermore, in view of the change from liquid healing agents to solid healed material, a mass exchange between these two constituents is introduced, dependent on the local concentration of catalysts. Finally, the applicability of the developed macroscopic four phase model is presented by means of a numerical example in comparison with an experiment.

1 INTRODUCTION

Traditionally, engineers design materials and structures in such a way that they have increased strength and stiffness in order to prevent damage and failures. But natural materials, like skin or tree bark, can deal with failures in a more efficient way: they heal by themselves. Inspired by these naturally self healing mechanisms, the field of research with respect to manufactured self healing materials growth steadily in the last years. For example, [1] developed a self healing system with microencapsulated healing agents and catalysts embedded in a polymer matrix. If a crack breaks through such a capsule, the healing agents flow into the crack and polymerize due to reaction with the embedded catalysts, which leads to the closure of the crack and, hence, regaining of a certain amount of strength and stiffness.

Regarding the numerical modeling of self healing polymer materials, some references will be introduced in the following.

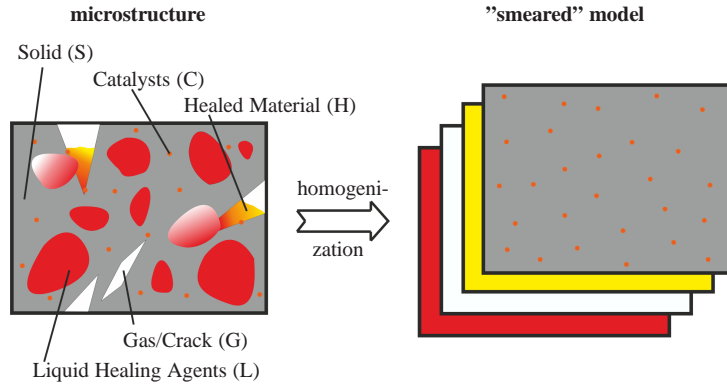


Figure 1: Homogenization of the microstructure.

Self healing effects of polymers in an analytical manner were analyzed by [2]. Regarding fiber reinforced composites the self healing behavior was investigated and simulated by [3–5]. In view of the development of thermodynamically consistent models it is referred to [6–8]. In [9] the simulations are based on Continuum Damage Mechanics (CDM), and [10] taking continuous damage and healing variables into account. The model of [11] is based on the Mixture Theory.

2 THEORETICAL FRAMEWORK

In order to describe the coupled multiphase problem the Theory of Porous Media (TPM) is used, which is a macroscopic continuum mechanical approach and combines the Mixture Theory with the Concept of Volume Fractions.

Within the Theory of Mixtures, all κ constituents φ^α , where α denotes the distinct phases of the model, are assumed to be statistically distributed over the observed volume. All different constituents φ^α appear in every material point \mathbf{X} of the observed volume simultaneously (superposition). Furthermore, the appearing geometrical and physical quantities are defined as statistically averages of the real quantities in the observed body. Using the Concept of Volume Fractions the different constituents in a material point can be identified by their volume fractions, i.e., the real quantities can be described in terms of partial quantities. Exemplary, the partial density ρ^α of a certain constituent can be directly related to its real density $\rho^{\alpha R}$ using the corresponding volume fraction $n^\alpha = dv^\alpha/dv$, such that $\rho^\alpha = n^\alpha \rho^{\alpha R}$. The sum over all κ volume fractions in a material point is restricted by the so called saturation condition

$$\sum_{\alpha=1}^{\kappa} n^\alpha = 1. \quad (1)$$

For a detailed discussion of the TPM, the interested reader is referred to BOWEN [12, 13], DE BOER [14, 15], EHLERS [16], and EHLERS & BLUHM [17].

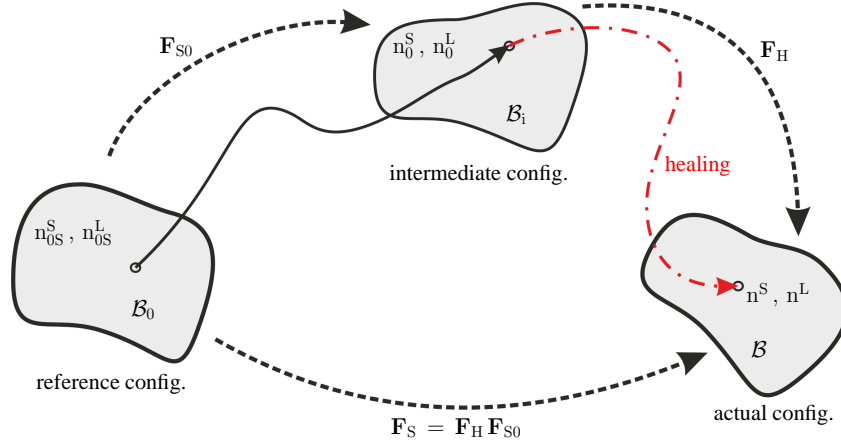


Figure 2: Illustration of the multiplicative decomposition of the deformation gradient corresponding to the solid phase.

3 SIMPLIFIED FOUR PHASE MODEL

Before we build up our four phase model, consisting of the solid matrix material (S) with dispersed catalysts (C), liquid healing agents (L), solid like healed material (H), and the gas phase (G), which represents the air, some assumptions are made: the influence of temperature is excluded; dynamic effects are neglected; a phase transition just happens between the liquid like healing agents and the solid like healed material; the gas phase is compressible, all other phases are incompressible; the volume fraction of catalysts is very small compared to the other phases, such it can be neglected with respect to the saturation condition.

Furthermore, it is assumed that the velocity of the solid and the healed material are identical and also the motion itself of these two phases are equal, except at an initial motion. This leads to a multiplicative decomposition of the deformation gradient, depicted in Figure 2, in the form

$$\mathbf{F}_S = \text{Grad } \chi_S = \frac{\partial \chi_S}{\partial \mathbf{X}_S} = \mathbf{F}_H \mathbf{F}_{S0} \quad (2)$$

proposed in [18–20]. Due to the multiplicative decomposition of the deformation gradient, three different right Cauchy-Green deformation tensors (solid, initial part of solid motion and healed material) are available,

$$\mathbf{C}_S = \mathbf{F}_S^T \mathbf{F}_S, \quad \mathbf{C}_{S0} = \mathbf{F}_{S0}^T \mathbf{F}_{S0}, \quad \hat{\mathbf{C}}_H = \mathbf{F}_H^T \mathbf{F}_H. \quad (3)$$

3.1 Field Equations

Under consideration of the above mentioned assumptions, the set of governing field equations are given by the balance equation of mass for the solid, healed material, liquid healing agents, catalysts and gas,

$$\begin{aligned}
 (n^S)'_S + n^S \operatorname{div} \mathbf{x}'_S &= 0, & (n^H)'_S + n^H \operatorname{div} \mathbf{x}'_S &= \frac{\hat{\rho}^H}{\rho^{\text{HR}}}, \\
 (n^L)'_L + n^L \operatorname{div} \mathbf{x}'_L &= -\frac{\hat{\rho}^H}{\rho^{\text{LR}}}, & n^S (c^C)'_S - \operatorname{div} (n^S c^C \mathbf{w}_{\text{CS}}) &= \hat{\rho}^C, \\
 (n^G)'_G + n^G \operatorname{div} \mathbf{x}'_G + \frac{n^G}{\rho^{\text{GR}}} (\rho^{\text{GR}})'_G &= 0,
 \end{aligned} \tag{4}$$

and the balance equations of momentum for the mixture as well as for the liquid and gas phases

$$\begin{aligned}
 \operatorname{div} \mathbf{T}^{\text{SHLG}} + \rho^{\text{SHLG}} \mathbf{b} &= -\hat{\rho}^H \mathbf{w}_{\text{LS}}, & \operatorname{div} \mathbf{T}^L + \rho^L \mathbf{b} &= -\hat{\mathbf{p}}^L, \\
 \operatorname{div} \mathbf{T}^G + \rho^G \mathbf{b} &= -\hat{\mathbf{p}}^G.
 \end{aligned} \tag{5}$$

The symbol $(\dots)'_\alpha$ indicates the material time derivative of the value with respect to the corresponding constituent α , whereas $(\hat{\dots})$ labels the direct production terms of mass and momentum, respectively. Here, the direct production terms of mass for the healed material ($\hat{\rho}^H$) and the catalysts ($\hat{\rho}^C$) depend on the concentration of the catalysts, whereas the direct production terms of momentum for liquid ($\hat{\mathbf{p}}^L$) and gas ($\hat{\mathbf{p}}^G$). The relative velocities with respect to the solid phase are defined by $\mathbf{w}_{\zeta S} = \mathbf{x}_\zeta - \mathbf{x}_S$. The value $c^C \in [0, 1]$ indicates the concentration of catalysts and $\mathbf{T}^\alpha = (\mathbf{T}^\alpha)^\top$ are the symmetric Cauchy stress tensors for the different constituents. The expressions \mathbf{T}^{SHLG} and ρ^{SHLG} describe the sum of the corresponding Cauchy stresses and partial densities, respectively, of the individual phases.

3.2 Constitutive Relations

In the following, the derivation of the constitutive relations for the Cauchy stresses and for the direct production terms of mass and momentum are briefly discussed following the thermodynamically consistent derivation of [21].

Due to the evaluation of the entropy inequality, the resulting restrictions with respect to the Cauchy stresses \mathbf{T}^α are given by

$$\begin{aligned}
 \mathbf{T}^{\text{SH}} &= -n^{\text{SH}} \lambda \mathbf{I} + \mathbf{T}_E^{\text{SH}}, & \mathbf{T}^L &= -n^L \lambda \mathbf{I} + \mathbf{T}_E^L, \\
 \mathbf{T}^G &= -n^G \lambda \mathbf{I} + \mathbf{T}_E^G, & \mathbf{T}^C &= \mathbf{T}_E^C,
 \end{aligned} \tag{6}$$

with the effective stress parts

$$\begin{aligned}
 \mathbf{T}_E^{\text{SH}} &= 2 \rho^S \mathbf{F}_S \frac{\partial \psi^S}{\partial \mathbf{C}_S} \mathbf{F}_S^\top + 2 \rho^H \mathbf{F}_H \frac{\partial \psi^H}{\partial \hat{\mathbf{C}}_H} \mathbf{F}_H^\top, & \mathbf{T}_E^L &= -n^L \rho^L \frac{\partial \psi^L}{\partial n^L} \mathbf{I}, \\
 \mathbf{T}_E^G &= -n^G \rho^L \frac{\partial \psi^L}{\partial n^G} \mathbf{I}, & \mathbf{T}_E^C &= -n^C \rho^C \frac{\partial \psi^C}{\partial n^C} \mathbf{I},
 \end{aligned} \tag{7}$$

and the Lagrange multiplier

$$\lambda = (\rho^{\text{GR}})^2 \frac{\partial \psi^{\text{G}}}{\partial \rho^{\text{GR}}} - \rho^{\text{L}} \frac{\partial \psi^{\text{L}}}{\partial n^{\text{G}}}. \quad (8)$$

The Lagrange multiplier is to be understood as a reaction force (pressure) on the rate of the saturation condition, which has to be considered with respect to the evaluation of the entropy inequality. A detailed discussion about the influence of the saturation condition on the constitutive relations can be found in [15].

Introducing the considered free Helmholtz energy functions for the different constituents

$$\begin{aligned} \psi^{\text{S}} &= \frac{1}{\rho_{0\text{S}}^{\text{SR}}} (1 - D^{\text{S}}) \left[\frac{1}{2} \lambda^{\text{S}} (\log J_{\text{S}})^2 - \mu^{\text{S}} \log J_{\text{S}} + \frac{1}{2} \mu^{\text{S}} (\mathbf{C}_{\text{S}} \cdot \mathbf{I} - 3) \right], \\ \psi^{\text{H}} &= \frac{1}{\rho_{0\text{H}}^{\text{HR}}} \epsilon^{\text{H}} (1 - D^{\text{H}}) \left[\frac{1}{2} \lambda^{\text{H}} (\log J_{\text{H}})^2 - \mu^{\text{H}} \log J_{\text{H}} + \frac{1}{2} \mu^{\text{H}} (\hat{\mathbf{C}}_{\text{H}} \cdot \mathbf{I} - 3) \right], \\ \psi^{\text{L}} &= \frac{1}{\rho_{0\text{L}}^{\text{LR}}} \left\{ k_{\text{h}}^{\text{L}} \left[-\text{dilog} \frac{1}{s^{\text{L}}} - \log \left(\frac{s_0^{\text{L}}}{s^{\text{L}}} - s_0^{\text{L}} \right) \log \frac{1}{s^{\text{L}}} + \log(1 - s_0^{\text{L}}) \log \frac{s_0^{\text{L}}}{s^{\text{L}}} \right. \right. \\ &\quad \left. \left. + \text{dilog} \frac{1}{s_0^{\text{L}}} + \log(1 - s_0^{\text{L}}) \log \frac{1}{s_0^{\text{L}}} \right] \right\}, \\ \psi^{\text{G}} &= -\Theta R^{\text{G}} \rho_{0\text{G}}^{\text{GR}} \rho^{\text{GR}} \left(\log \frac{\rho_{0\text{G}}^{\text{GR}}}{\rho^{\text{GR}}} - \frac{\rho_{0\text{G}}^{\text{GR}}}{\rho^{\text{GR}}} + 1 \right) + p_0^{\text{GR}} \rho^{\text{GR}}, \\ \psi^{\text{C}} &= \frac{1}{\rho_{0\text{C}}^{\text{CR}}} \left[\frac{1}{2} k^{\text{C}} \log \frac{1}{c^{\text{C}}} - p_0^{\text{CR}} \log \frac{1}{c^{\text{C}}} \right], \end{aligned} \quad (9)$$

the constitutive relations for the Cauchy stresses read

$$\begin{aligned} \mathbf{T}^{\text{SH}} &= -n^{\text{SH}} \lambda \mathbf{I} + \frac{1}{J_{\text{S}}} \left\{ (1 - D^{\text{S}}) [2\mu^{\text{S}} \mathbf{K}_{\text{S}} + \lambda^{\text{S}} (\log J_{\text{S}}) \mathbf{I}] + \right. \\ &\quad \left. + \epsilon^{\text{H}} n^{\text{H}} J_{\text{S}} (1 - D^{\text{H}}) [2\mu^{\text{H}} \mathbf{K}_{\text{H}} + \lambda^{\text{H}} (\log J_{\text{H}}) \mathbf{I}] \right\}, \\ \mathbf{T}^{\text{L}} &= -n^{\text{L}} p^{\text{LR}} \mathbf{I}, \quad \mathbf{T}^{\text{G}} = -n^{\text{G}} p^{\text{GR}} \mathbf{I}, \quad \mathbf{T}^{\text{C}} = -n^{\text{C}} p^{\text{CR}} \mathbf{I}. \end{aligned} \quad (10)$$

Here, λ^{S} , μ^{S} and λ^{H} , μ^{H} are the Lamé constants of the solid and healed material phase. The parameter ϵ^{H} is chosen in such a way that the product $\epsilon^{\text{H}} n^{\text{H}}$ is equal to one if the liquid like healing agents are completely transformed into solid healed material. This ensures that the healed material comes full into play only if the structure is totally healed in this material point. The Karni-Reiner strain tensors of the solid and healed material are given by $\mathbf{K}_{\text{S}} = \frac{1}{2}(\mathbf{B}_{\text{S}} - \mathbf{I})$ and $\mathbf{K}_{\text{H}} = \frac{1}{2}(\mathbf{B}_{\text{H}} - \mathbf{I})$, where $\mathbf{B}_{\text{S}} = \mathbf{F}_{\text{S}} \mathbf{F}_{\text{S}}^{\text{T}}$ and $\mathbf{B}_{\text{H}} = \mathbf{F}_{\text{H}} \mathbf{F}_{\text{H}}^{\text{T}}$ are the left Cauchy-Green strain tensors of the solid and healed material.

In order to describe the damage behavior of both, the solid and healed material independently, two different damage functions are introduced. Here, the so called $(1 - D)$ approach, introduced in [22], is used. For a detailed discussion of this discontinuous damage model see also [23, 24].

The Lagrange multiplier λ consists of the real gas pressure p^{GR} and an additional pressure part, in the following denoted by p^{h} , aligned to the capillary pressure presented in [21], depending on the liquid saturation,

$$\lambda = p^{\text{GR}} - p^{\text{h}}, \quad (11)$$

wherein p^{h} is defined as

$$p^{\text{h}} = k_{\text{h}}^{\text{L}} s^{\text{L}} \left[\log \left(\frac{s_0^{\text{L}}}{s^{\text{L}}} - s_0^{\text{L}} \right) - \log (1 - s_0^{\text{L}}) \right]. \quad (12)$$

The constants k_{h}^{L} and s_0^{L} are material parameters and the liquid saturation $s^{\text{L}} = n^{\text{L}}/(n^{\text{L}} + n^{\text{G}})$ is the ratio of liquid with respect to the whole hollow space inside the observed body. Furthermore, the real gas pressure is described by the nonlinear gas law

$$p^{\text{GR}} = -\Theta R^{\text{G}} \rho_{0\text{G}}^{\text{GR}} \log \frac{\rho_{0\text{G}}^{\text{GR}}}{\rho^{\text{GR}}} + p_0^{\text{GR}}, \quad (13)$$

where Θ is the absolute temperature, R^{G} denotes the specific gas constant, $\rho_{0\text{G}}^{\text{GR}}$ and p_0^{GR} are initial real gas density and the initial real gas pressure. The real liquid pressure p^{LR} is also described by a saturation dependent function given as

$$p^{\text{LR}} = p^{\text{GR}} + k_{\text{h}}^{\text{L}} \left[\log \left(\frac{s_0^{\text{L}}}{s^{\text{L}}} - s_0^{\text{L}} \right) - \log (1 - s_0^{\text{L}}) \right], \quad (14)$$

see also [21]. Finally, the last pressure part of Eq. (10) is the real pressure of catalysts, which is given by

$$p^{\text{CR}} = -k^{\text{C}} \log \frac{1}{c^{\text{C}}} + p_0^{\text{CR}}, \quad (15)$$

whereat the concentration is defined as the quotient of volume fractions of catalysts and solid $c^{\text{C}} = n^{\text{C}}/n^{\text{S}}$.

In order to describe the mass exchange between the liquid healing agents and the solid healed material an ansatz for the production term of healed material. Therefore, the production function proposed in [25] is used. Here, this function is modified such that it depends on the concentration of catalysts,

$$\hat{\rho}^{\text{H}} = \hat{\rho}_{\text{m}}^{\text{H}} \left(\frac{c^{\text{C}} - c_0^{\text{C}}}{c_{\text{m}}^{\text{C}}} \right)^2 \exp \left[1 - \left(\frac{c^{\text{C}} - c_0^{\text{C}}}{c_{\text{m}}^{\text{C}}} \right)^2 \right]. \quad (16)$$

Therein, $\hat{\rho}_{\text{m}}^{\text{H}}$ is the maximum value of $\hat{\rho}^{\text{H}}$ and c_0^{C} the maximum value of the concentration. The value c_{m}^{C} denotes the change of concentration where $\hat{\rho}^{\text{H}}$ becomes its maximum.

Due to the fact that the concentration of catalysts decrease in the areas where healing occur, the total production term of mass for the catalysts $\hat{\rho}^{\text{C}}$ is negative and set to be constant. Furthermore, due to the evaluation of the entropy inequality, the direct production terms of momentum for liquid and gas are given by

$$\begin{aligned}\hat{\mathbf{p}}^L &= \lambda \operatorname{grad} n^L - p^h \operatorname{grad} n^G + \hat{\mathbf{p}}_E^L, \\ \hat{\mathbf{p}}^G &= (\lambda + p^h) \operatorname{grad} n^G - \hat{\mathbf{p}}_E^G.\end{aligned}\quad (17)$$

In Eq. (17) the vectors

$$\hat{\mathbf{p}}_E^L = -\gamma_{\mathbf{w}_{LS}}^L \mathbf{w}_{LS} - \gamma_{\mathbf{w}_{GS}}^L \mathbf{w}_{GS}, \quad \hat{\mathbf{p}}_E^G = -\gamma_{\mathbf{w}_{GS}}^G \mathbf{w}_{GS} - \gamma_{\mathbf{w}_{LS}}^G \mathbf{w}_{LS} \quad (18)$$

denote the effective parts of the direct production terms of momentum, whereat the occurring material parameters are restricted by

$$\gamma_{\mathbf{w}_{LS}}^L \geq 0, \quad \gamma_{\mathbf{w}_{GS}}^G \geq 0, \quad \gamma_{\mathbf{w}_{GS}}^L + \gamma_{\mathbf{w}_{LS}}^G = 0. \quad (19)$$

4 NUMERICAL EXAMPLE

In order to show the applicability of the developed model, a numerical simulation of a real experiment, cp. [26], is carried out. The dimensions of the specimen and the damaged virtual specimen are depicted in Figure 3. Here, the virtual specimen is discretized with 142 linear

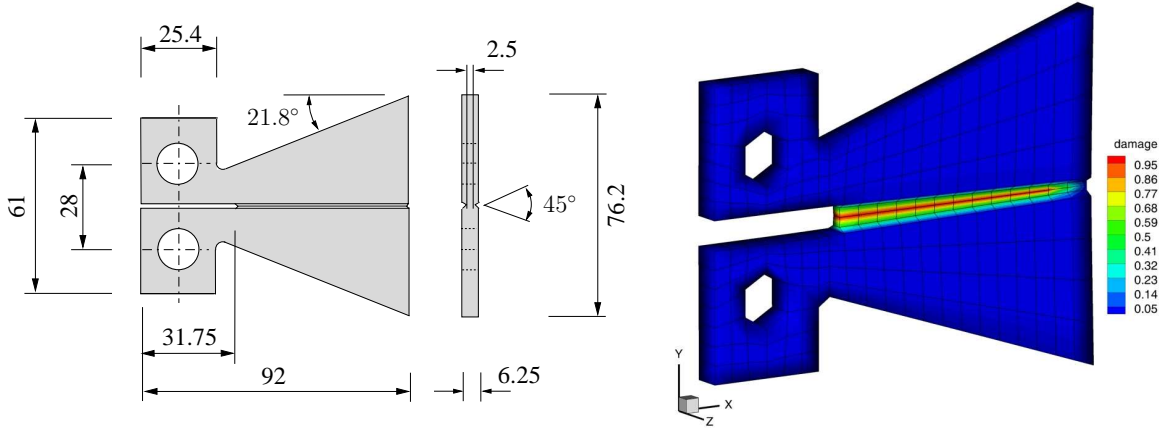


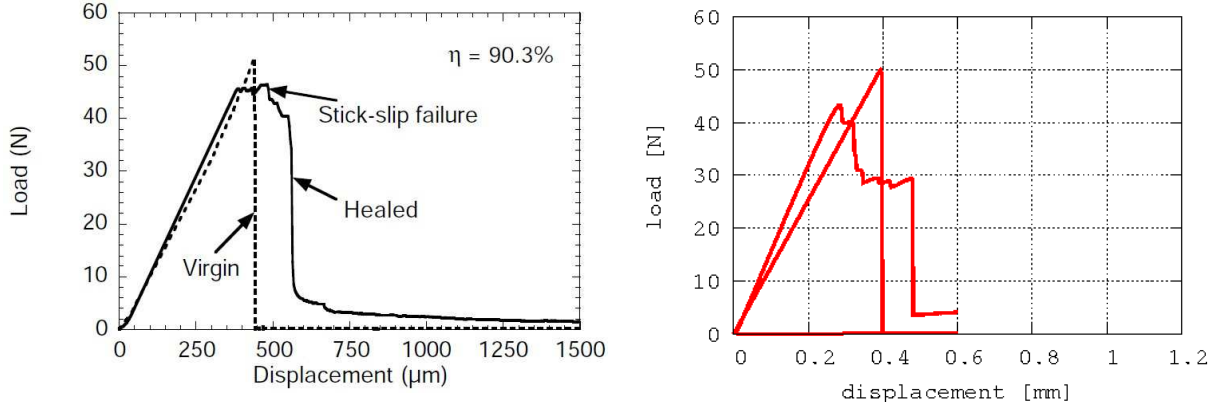
Figure 3: TDCB geometry, cp. [26] (left); damaged virtual specimen (right).

eight-nodular brick elements and the total number of degrees of freedom is 2492. On both flanks a displacement of $u = 0.6$ mm is applied in y -direction. Moreover, the boundary surface at the beginning of the notch is open for the gas phase, i.e., air can flow in and out.

During the loading the TDCB fails. After that, the specimen is unloaded, because in the experiment the specimen is also just able to heal, if the crack faces come into contact. Then, the TDCB gets 48 hours resting time before it is reloaded. As it is depicted in Figure 4, the results of the numerical simulation is qualitatively in a very good agreement to the experimental results.

Table 1: Initial material parameters.

| | S | H | L | G | C | unit |
|---|--------|--------|--------|--------|-----|---------------------|
| Young's modulus E^α | 3.0e+9 | 3.0e+9 | – | – | – | Pa |
| Poisson's ratio ν^α | 0.2 | 0.2 | – | – | – | – |
| real density $\rho_{0\alpha}^{\alpha R}$ | 1200.0 | 980.0 | 980.0 | 1.0 | – | kg/m ³ |
| Darcy parameter k_{Darcy}^α | – | – | 9.0e-9 | 5.0e+2 | – | m ⁴ /N s |
| Parameter associated with healing k_h^L | – | – | 5.0e+1 | – | – | Pa |
| initial volume fraction n^α | 0.7 | 0.0 | 0.2 | 0.1 | – | – |
| initial concentration c_0^α | – | – | – | – | 1.0 | ×100% |
| initial saturation s_0^L | – | – | 0.9 | – | – | – |

**Figure 4:** Experimental result, cp. [26] (left); result of the numerical simulation (right).

5 CONCLUSION

The presented work concentrates on the numerical simulation of damage as well as healing effects in a self-healing polymer composite. As the underlying theoretical framework the Theory of Porous Media is used. The developed multiphase model consists of the solid matrix material with dispersed catalysts, the liquid like healing agents, the solid like healed material, and the gas phase. For the separate description of damage for the solid and the healed material, two different damage functions are introduced based on the $(1 - D)$ approach. In order to describe the healing mechanism, a phase transition between the liquid healing agents and the solid healed material is considered.

To show the applicability of the developed model, the numerical simulation of a tapered double cantilever beam (TDCB) is compared with the experimental result from [26]. The simulation shows a qualitatively good agreement with the experimental observation, even for the healing efficiency. The divergence between both results can be explained, e.g., due to the fact that the healing of the real specimen depends on different factors, like wetting, different distributions of microcapsules and catalysts in the damaged area, etc.. Hence, it can be assumed that

the resulting load-displacement curves of different specimens vary.

As next step, the model should be extended in order to describe also fiber reinforced composites (FRCs), which are of great interest in the fields of, e.g. aerospace or wind power plants.

Acknowledgements This work has been supported by the German Research Society (DFG) within the Priority Program SPP 1568 “Design and Generic Principles of Self-healing Materials” under the grant number BL 417/7-1.

REFERENCES

- [1] White, S.R., Sottos, N.R., Geubelle, P.H., Moore, J.S., Kessler, M.R., Sriram, S.R., Brown, E.N. and Viswanathan, S. Autonomic healing of polymer composites. *Nature* (2001) **409**:794–797.
- [2] Zemskov, S.V., Jonkers, H.M. and Vermolen, F.J. Two analytical models for the probability characteristics of a crack hitting encapsulated particles: application to self-healing materials. *Computational Materials Science* (2011) **50**:3323–3333.
- [3] Sanada, K., Itaya, N. and Shindo, Y. Self-healing of interfacial debonding in fiber-reinforced polymers and effect of microstructure on strength recovery. *The Open Mechanical Engineering Journal* (2008) **2**:97–103.
- [4] Barbero, E.J. and Ford, K.J. Characterization of self-healing fiber-reinforced polymer-matrix composite with distributed damage. *Journal of Advanced Materials* (2007) **39**:20–27.
- [5] Privman, V., Dementsov, A. and Sokolov, I. Modeling of self-healing polymer composites reinforced with nanoporous glass fibers. *Journal of Computational and Theoretical Nanoscience* (2007) **4**:190–193.
- [6] Voyiadjis, G.Z., Shojaei, A. and Li, G. A thermodynamic consistent damage and healing model for self healing materials. *International Journal of Plasticity* (2011) **27**:1025–1044.
- [7] Yagimli, B. and Lion, A. Experimental investigations and material modelling of curing processes under small deformations. *Zeitschrift für angewandte Mathematik und Mechanik* (2011) **91**:342–359.
- [8] Schimmel, E.C. and Remmers, J.J.C. *Development of a constitutive model for self-healing materials*. Tech. Report, Delft Aerospace Computational Science, (2006).
- [9] Voyiadjis, G.Z., Shojaei, A., Li, G. and Kattan, P.I. A theory of anisotropic healing and damage mechanics of materials. *Proceedings of the Royal Society London A* (2012) **468**:163–183.

- [10] Mergheim, J. and Steinmann, P. Phenomenological modelling of self-healing polymers based on integrated healing agents. *Computational Mechanics* (2013) DOI 10.1007/s00466-013-0840-0.
- [11] Henson, G.M. Engineering models for synthetic vascular materials with interphase mass, momentum and heat transfer. *International Journal of Solids and Structures* (2012), submitted.
- [12] Bowen, R.M. Incompressible porous media models by use of the theory of mixtures. *Int. J. Eng. Sci.* (1980) **18**:1129–1148.
- [13] Bowen, R.M. Compressible porous media models by use of the theory of mixtures. *Int. J. Eng. Sci.* (1982) **20**:697–735.
- [14] de Boer, R. *Trends in continuum mechanics of porous media*. Springer, (2005).
- [15] de Boer, R. *Theory of porous media*. Springer, (2000).
- [16] Ehlers, W. *Poröse Medien - ein kontinuummechanisches Modell auf der Basis der Mischungstheorie*. PhD.-Thesis, Universität - Gesamthochschule - Essen, (1989).
- [17] Ehlers, W. and Bluhm, J. (ed.), *Porous media*. Springer, (2002).
- [18] Ateshian, G.A. and Ricken, T. Multigenerational interstitial growth of biological tissues, *Biomechanics and Modelling in Mechanobiology* (2010) **9**:689–702.
- [19] Hunphrey, J. and Rajagopal, K. A constrained mixture model for growth and remodelling of soft tissues, *Mathematical Models and Methods in Applied Science* (2002) **12**:407–430.
- [20] Rodriguez, E., Hoger, A. and McCulloch, A. Stress-dependent finite growth in soft elastic tissues, *Journal of Biomechanics* (1994) **27**:455–467.
- [21] Bluhm, J., Ricken, T. and Bloßfeld, W.M. Ice formation in porous media, in *Advances in extended & multifield theories for continua*. Markert, B. (ed.) Springer, (2011).
- [22] Kachanov, L.M. Time of the rupture process under creep conditions, *Izvestija Akademii Nauk Sojuza Sovetskich Socialisticeskich Republiki (SSSR) Otdelenie Techniceskich Nauk (Moskra)* (1958) **8**:26–31.
- [23] Miehe, C. Discontinuous and continuous damage evolution in Ogden-type large-strain elastic materials, *European Journal of Mechanics, A/Solids* (1995) **14**:697–720.
- [24] Balzani, D. *Polyconvex anisotropic energies and modeling of damage applied to arterial walls*. PhD.-Thesis, Universität Duisburg-Essen, (2006).

- [25] Michalowski, R.L. and Zhu, M. Frost heave modelling using porosity rate function, *International Journal for Numerical and Analytical Methods in Geomechanics* (2006) **30**:703–722.
- [26] Brown, E.N., Sottos, N.R. and White, S.R. Fracture testing of a self-healing polymer composite, *Experimental Mechanics* (2002) **42**:372–379.